

46  
1  
Grant NGR-05-020-102 27

3 THEORETICAL STUDIES OF SOME NONLINEAR  
ASPECTS OF HYPERSONIC PANEL FLUTTER 4

Stanford University 3

4 STATUS REPORT NUMBER 4

71 March 1967 to 31 August 1967 6 CV 110

FACILITY FORM 602	N67-39328	
	(ACCESSION NUMBER)	(THRU)
	10/4/22-26	7
	(PAGES)	(CODE)
	CR-89268 END	32
	(NASA CR OR TMX OR AD NUMBER)	(CATEGORY)

## NOTATION

$a$	Panel chord
$D$	Panel stiffness parameter, $Eh^3/12(1-\nu^2)$
$h$	Panel thickness
$K$	Spring constant (per unit span)
$M$	Mach number of free stream
$p$	Pressure; $p_\infty$ is that of free stream
$\Delta p$	Static pressure difference across panel; $\tilde{\Delta p} = \Delta p a^4/Dh$
$q$	Free-stream dynamic pressure, $\rho U^2/2$
$R_x$	Dimensionless in-plane applied load, $F_x a^2/D$
$t$	Time
$U$	Free-stream speed
$w$	Dimensionless panel transverse displacement, $\bar{w}/h$
$x$	Chordwise panel coordinate
$\alpha$	Panel in-plane restraint parameter, $Ka/[Ka(1-\nu^2) + Eh]$
$\lambda$	Dynamic-pressure parameter, $2qa^3/MD$
$\mu$	Aerodynamic damping parameter, $\rho a/\rho_m h$
$\xi$	Dimensionless chordwise coordinate, $x/a$
$\rho$	Free-stream density
$\rho_m$	Panel density
$\tau$	Dimensionless time, $t(D/\rho_m h a^4)^{1/2}$

## Project Status

### EFFECT OF AERODYNAMIC NONLINEARITY (PANEL ON HINGED SUPPORTS):

Consider the two-dimensional panel, or plate-column, illustrated in Fig. 1. The supports are hinged, and their in-plane motion is resisted by a distributed spring whose running spring constant is  $K$ . Free-stream parameters shown are the Mach number  $M$  and dimensionless dynamic pressure  $\lambda$ . The panel is loaded by an applied in-plane load,  $R_x$ , a static pressure difference,  $\Delta p$ , and an unsteady pressure difference  $p - p_\infty$ . The unsteady pressure is approximated in hypersonic flow by the second-order piston-theory expression

$$p - p_\infty = \frac{2q}{M} \left\{ \frac{1}{U} \frac{\partial \bar{w}}{\partial t} + \frac{\partial \bar{w}}{\partial x} + \frac{(\gamma+1)M}{4} \left[ \frac{1}{U^2} \left( \frac{\partial \bar{w}}{\partial t} \right)^2 + \frac{2}{U} \frac{\partial \bar{w}}{\partial x} \frac{\partial \bar{w}}{\partial t} + \left( \frac{\partial \bar{w}}{\partial x} \right)^2 \right] \right\} \quad (1)$$

Here  $\bar{w}(x, t)$  is the middle-surface transverse displacement of the panel, and  $q$  is the free-stream dynamic pressure. Since the pressure acts normal to the instantaneous panel surface, there arise in a rigorous sense both transverse and in-plane aerodynamic loads when the plate deflection becomes finite. Order-of-magnitude consistency then dictates including both a transverse aerodynamic load  $p - p_\infty + \Delta p$  and an in-plane aerodynamic load  $[(p - p_\infty)_L + \Delta p] \cdot \frac{\partial \bar{w}}{\partial x}$ ; the subscript "L" on the unsteady pressure term in the latter expression denotes the linear terms of Eq. (1). The panel transverse displacement is assumed as a series

$$\bar{w}(x, t) = \sum_{k=1}^N \bar{a}_k(t) \sin \frac{k\pi x}{a} \quad (2)$$

which satisfies (at least) the geometric constraints on the panel. Using the assumed form of Eq. (2), aerodynamic loads from Eq. (1), and the method of solution described in Ref. 1 produces the following set of equations for the unknown coefficients  $a_k = \bar{a}_k/h$ :

$$\begin{aligned}
& \frac{1}{2} \frac{d^2 a_k}{d\tau^2} + \frac{\pi^2 k^2}{2} (R_x + \pi^2 k^2) a_k + \frac{3}{2} \pi^4 k^2 \alpha (1 - \nu^2) a_k \sum_{\ell=1}^N \ell^2 a_\ell^2 \\
& + \lambda \sum_{\ell=1}^N \frac{k\ell [1 - (-1)^{k+\ell}]}{k^2 - \ell^2} a_\ell + \frac{1}{2} \left( \frac{\mu\lambda}{M} \right)^{1/2} \frac{da_k}{d\tau} + \frac{1}{k\pi} [1 - (-1)^k] \tilde{\Delta p} \\
& + A \left( \lambda M \frac{h}{a} \right) \left[ \cdots \left( \frac{\partial \bar{w}}{\partial x} \right)^2 \cdots \right] + B \left( \frac{h}{a} \right) (\mu M \lambda)^{1/2} \left[ \cdots \left( \frac{\partial \bar{w}}{\partial x} \frac{\partial \bar{w}}{\partial t} \right) \cdots \right] \\
& + C \left( \mu \frac{h}{a} \right) \left[ \cdots \left( \frac{\partial \bar{w}}{\partial t} \right)^2 \cdots \right] + D \left( \lambda \frac{h^2}{a} \right) \left[ \cdots \left( \frac{\partial \bar{w}}{\partial x} \frac{\partial \bar{w}}{\partial t} \right) \cdots \right] \\
& + E \left( \frac{h^2}{a} \right) \left( \frac{\mu\lambda}{M} \right)^{1/2} \left[ \cdots \left( \frac{\partial \bar{w}}{\partial x} \right)^2 \cdots \right] + F \left( \frac{h^2}{a} \right) \left[ \cdots \left( \tilde{\Delta p} \frac{\partial \bar{w}}{\partial x} \right) \cdots \right] \\
& = 0, \quad k = 1, 2, \dots, N
\end{aligned} \tag{3}$$

The first six terms in these equations are those associated with linear aerodynamic theory and nonlinear structural theory, as found, for example, in Ref. 2. The structural nonlinearity — that associated with in-plane stretching — manifests itself as the term of third order in the  $a_k$ . Because of its stabilizing effect, it is known as a "hard" nonlinearity. The terms arising from the aerodynamic nonlinearity are those prefaced by the letters A through F. The

parameters involved in these terms are given as they actually appear, but the remainder of these terms are shown symbolically for the sake of brevity. The expressions in the brackets identify the origin of the nonlinear terms. Thus the terms labeled A, B, and C represent the contribution from the nonlinear part of the transverse aerodynamic loading, while those labeled D, E, and F result from the inclusion of an in-plane aerodynamic load. In contrast to the structural nonlinearity, these terms are quadratic in the  $a_k$  and their derivatives, and because of their destabilizing effect they are known as "soft" nonlinearities.

Eqs. (3) are solved by prescribing appropriate initial conditions – values for the  $a_k$  and  $\frac{da_k}{d\tau}$  at  $\tau = 0$  – and integrating to get the  $a_k$  as functions of time. The coefficients A through F can be chosen as zero or unity in the computer program, so that each of the aerodynamic nonlinear terms can be evaluated separately if desired.

The computer program was first checked by running some cases comparable to those given in Ref. 2. The results were in close agreement. This phase of the investigation led to some interesting and unanticipated problems when the equations were solved for zero system damping ( $\mu = 0$ ). Figures 2 and 3, for example, show the dimensionless panel displacement at the three-quarter chord vs. dimensionless time for one set of initial conditions –  $a_1(0) = 0.1$ , all other  $a_k(0)$  and  $\frac{da_k}{d\tau}(0)$  equal to zero. The value of  $\lambda$  chosen is supercritical for this configuration;  $\alpha = 1.0$  gives essentially a panel with infinite in-plane restraint, and none of the nonlinear aerodynamic terms were

included. After an initial transient, the panel response continues without change periodically, but not in simple harmonic motion. The response is different for different initial conditions, as is evidenced by Fig. 4, and the peak amplitudes are different. (The motion shown in Fig. 4 is also repeated without change.) This is not to say, however, that there is no unique limit-cycle amplitude associated with zero system damping. For the two-mode case, limit-cycle values for  $a_1$  and  $a_2$  at zero damping were available from an independent calculation; with these values used as initial conditions, the response curve of Fig. 5 was obtained. Here the response is regular, and the amplitude remains constant. It appears then that with zero damping the panel will oscillate between an unstable state and a stable state unless the initial conditions are such as to put it on the boundary between the two states. In Fig. 4, for example, the panel is clearly unstable initially, but after the amplitude reaches a certain point it becomes stable, to the extent that the amplitude drops into the unstable region again. In order to verify these conjectures, the computer program is being modified so that the energy of the panel and the work done by the aerodynamic forces can also be calculated as functions of time.

Aerodynamic nonlinearities were then introduced into the problem. One effect of these "soft" nonlinearities is the possibility of amplitude-sensitive flutter. This effect is illustrated in Figs. 6 and 7. At a subcritical value of  $\lambda$ , one set of initial data leads to a stable response (Fig. 6), while slightly increasing the initial amplitude leads to an unstable response. Here an additional system parameter,  $Mh/a$ , must be specified. Note also that the in-plane

restraint parameter  $\alpha$  is set to zero, thereby eliminating the stabilizing effect of the structural nonlinearity. It is interesting to note that additional runs to date with even very small values of  $\alpha$  have all produced stable panel responses with the same system parameters used for Figs. 6 and 7. Apparently the stabilizing effect of the structural nonlinearity is quite strong for all nonzero values of  $\alpha$ . It is again clear that more information on the energy interchange between panel and free stream would be most useful, not only in understanding better the amplitude-sensitive instability but also in predicting the impact of aerodynamic nonlinearities on supercritical panel response, which is of course of more practical interest.

#### CLAMPED PANEL WITH VARYING END LOAD:

No numerical results have yet been obtained. Some delays are anticipated because of changes in computer equipment at the Stanford Computation Center (see below).

#### COMPUTING:

The Stanford Computation Center has recently acquired an IBM 360/67 computer. It will therefore be necessary to do a certain amount of reprogramming in order to utilize this computer to its full capacity. It is proposed to do all future programming in Fortran IV, Level H, so that the programs might be of value at other computer installations.

#### ANNUAL REPORT:

An annual report on the year's activities is being prepared.

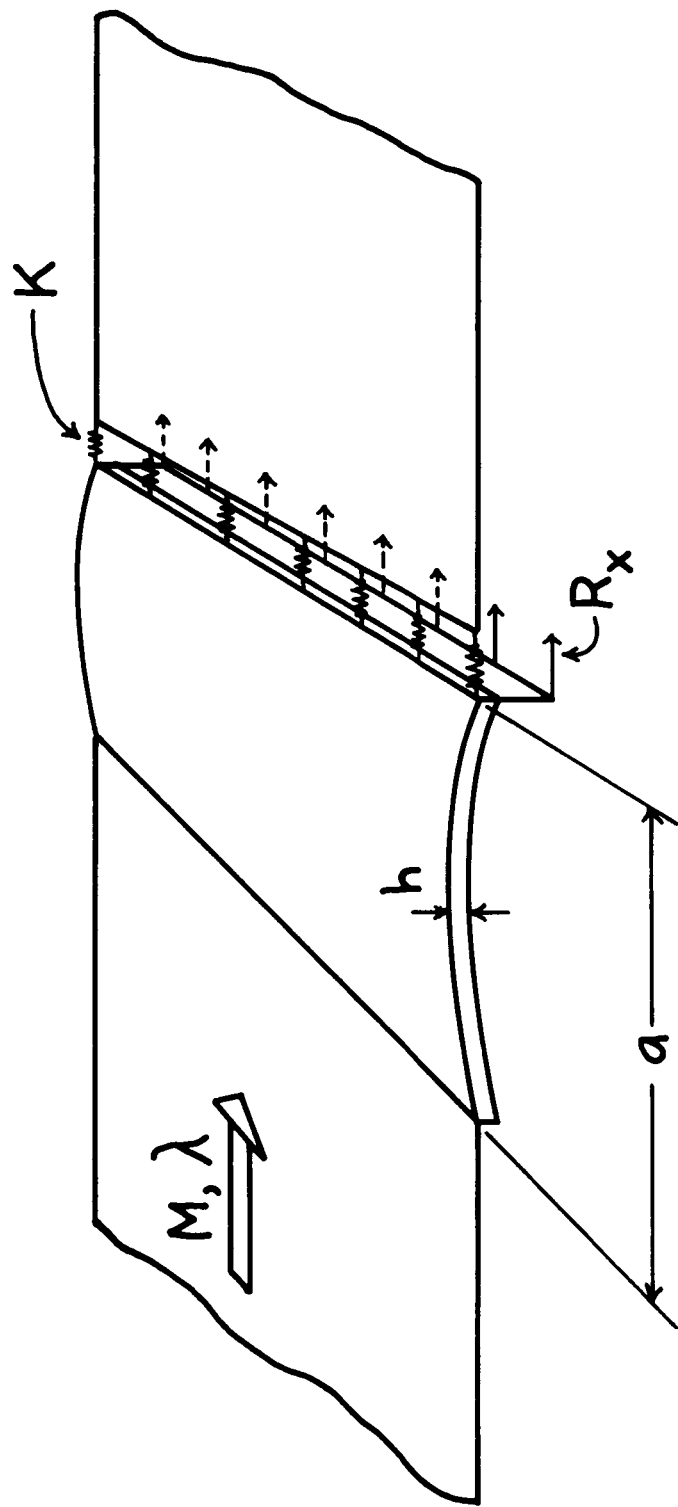


Figure 1. Panel (plate-column) on hinged supports



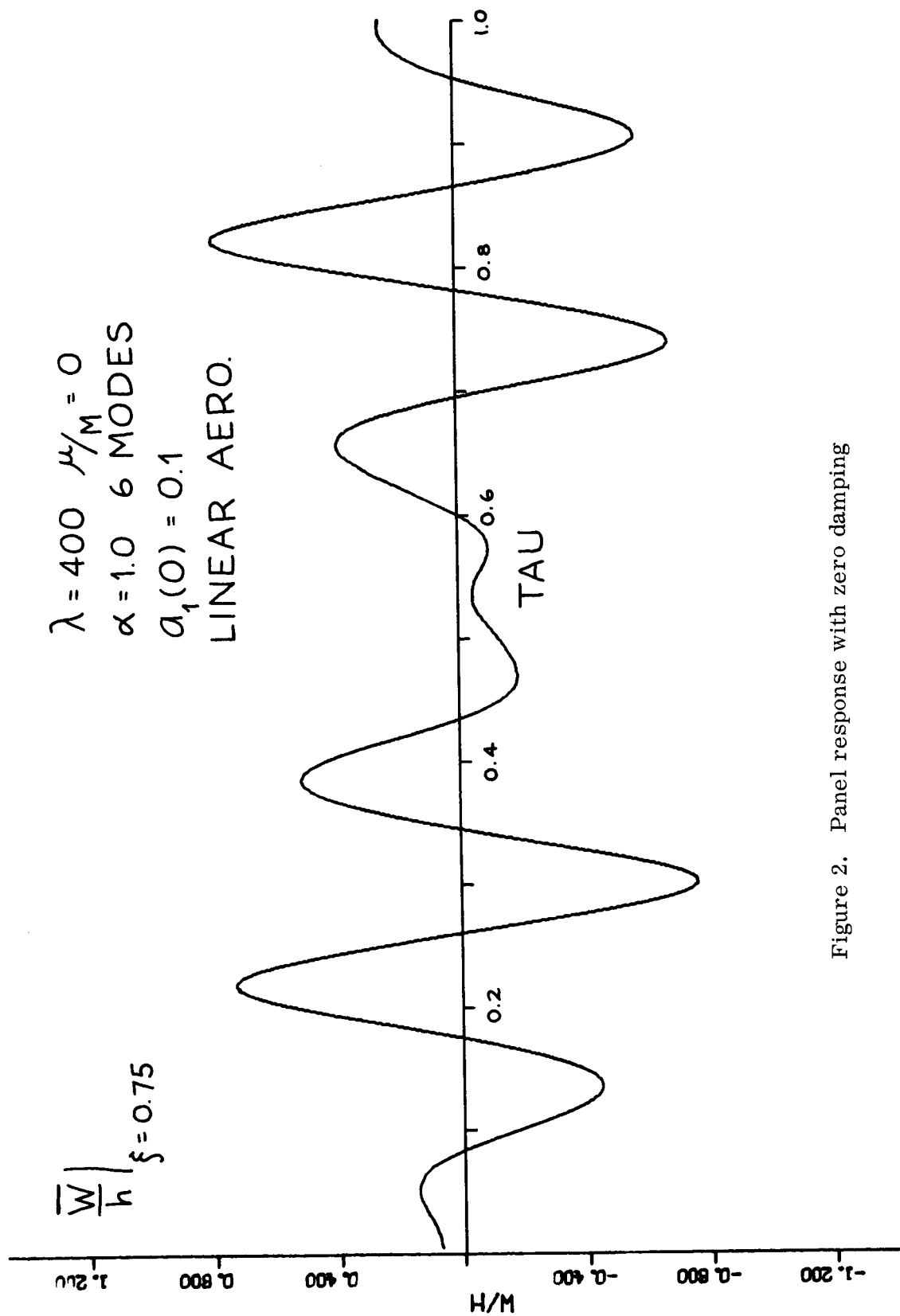


Figure 2. Panel response with zero damping

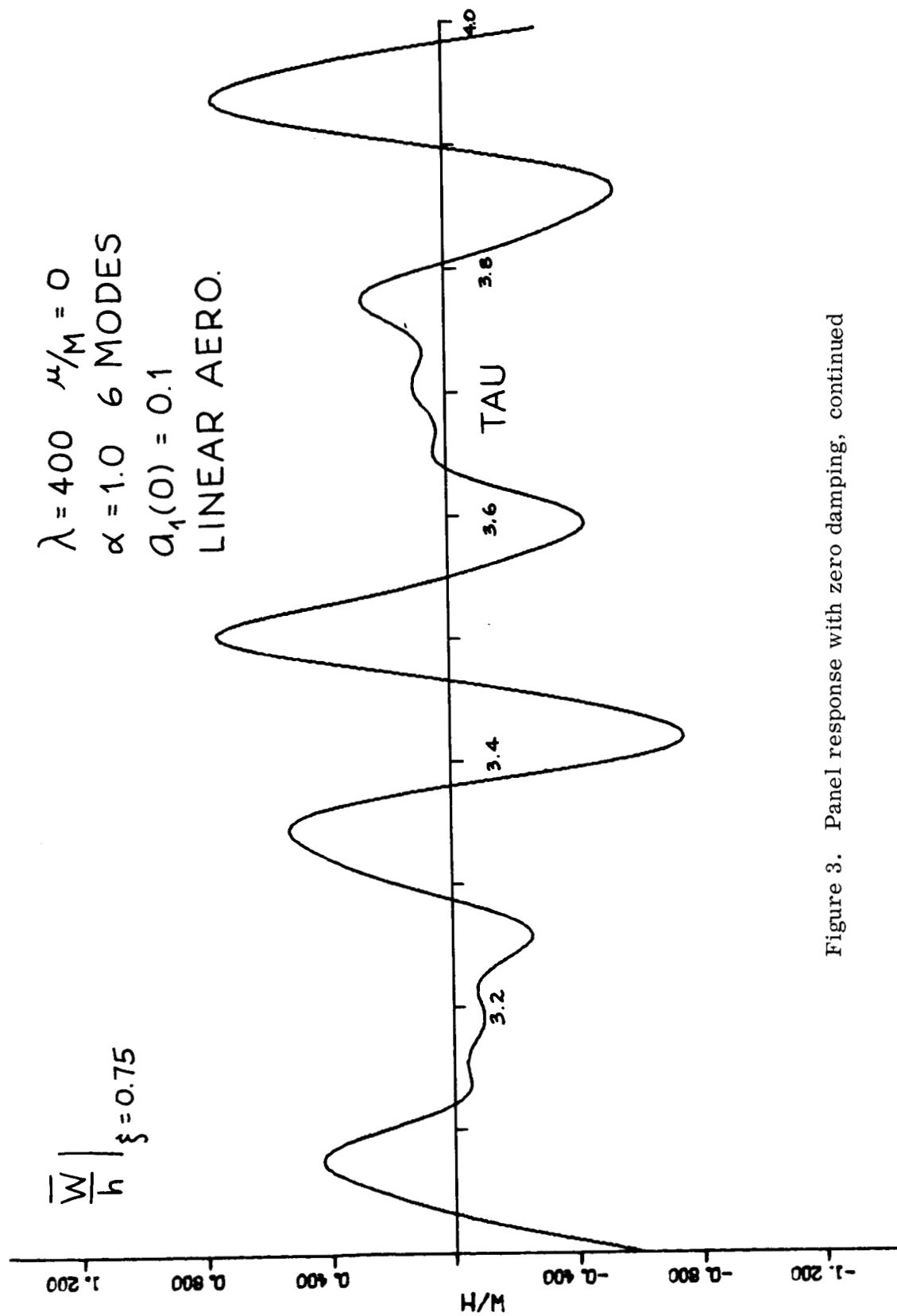


Figure 3. Panel response with zero damping, continued

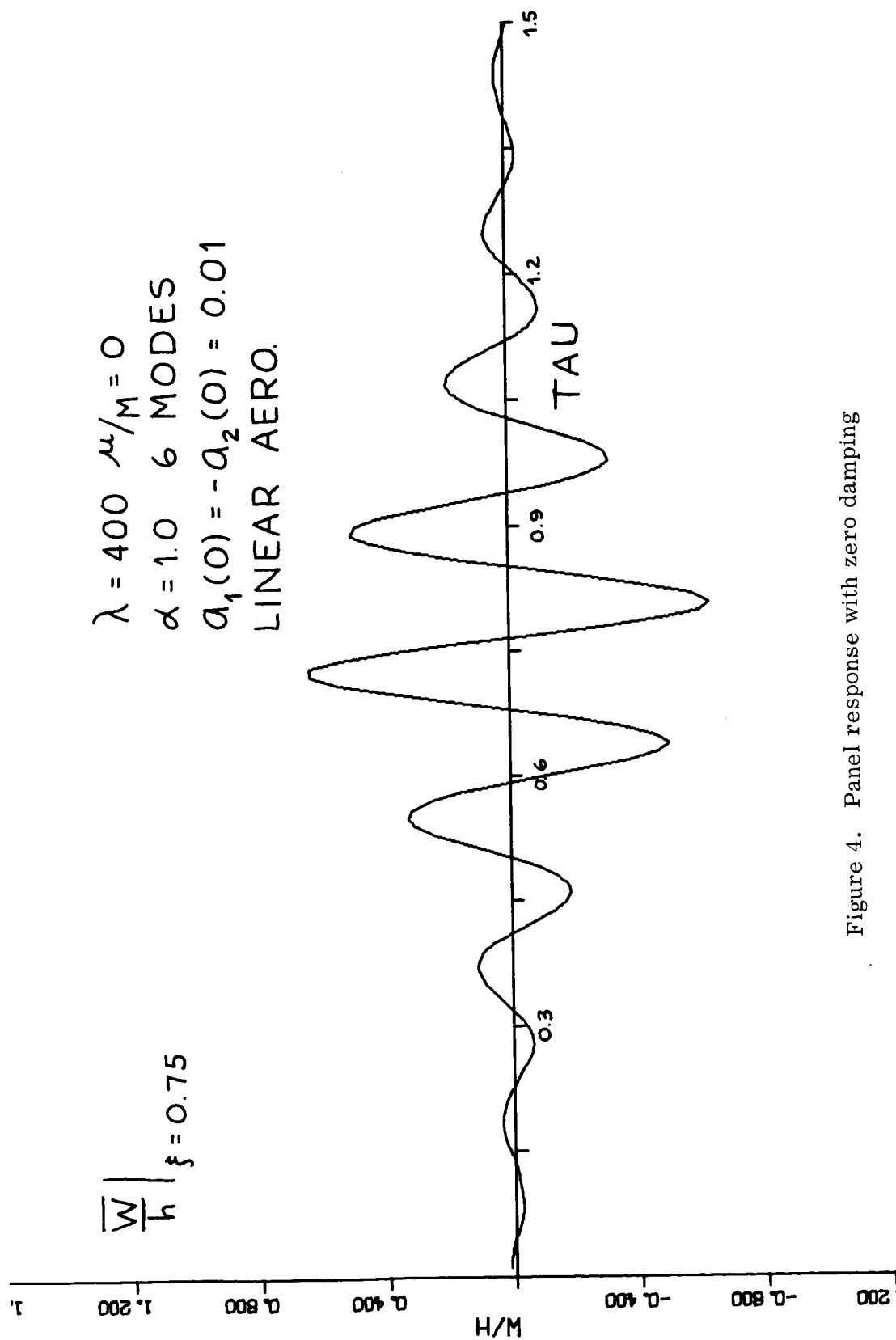


Figure 4. Panel response with zero damping

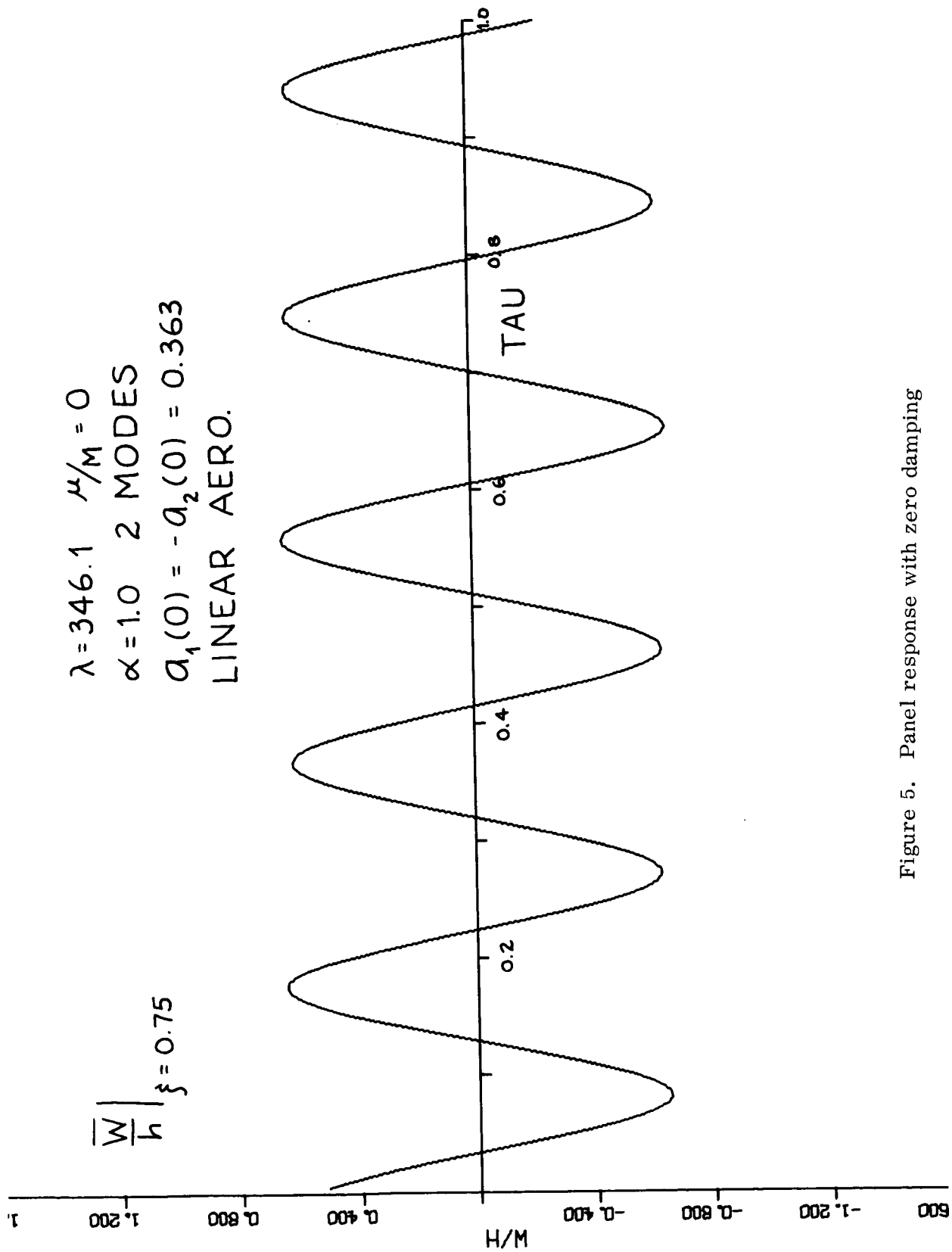


Figure 5. Panel response with zero damping

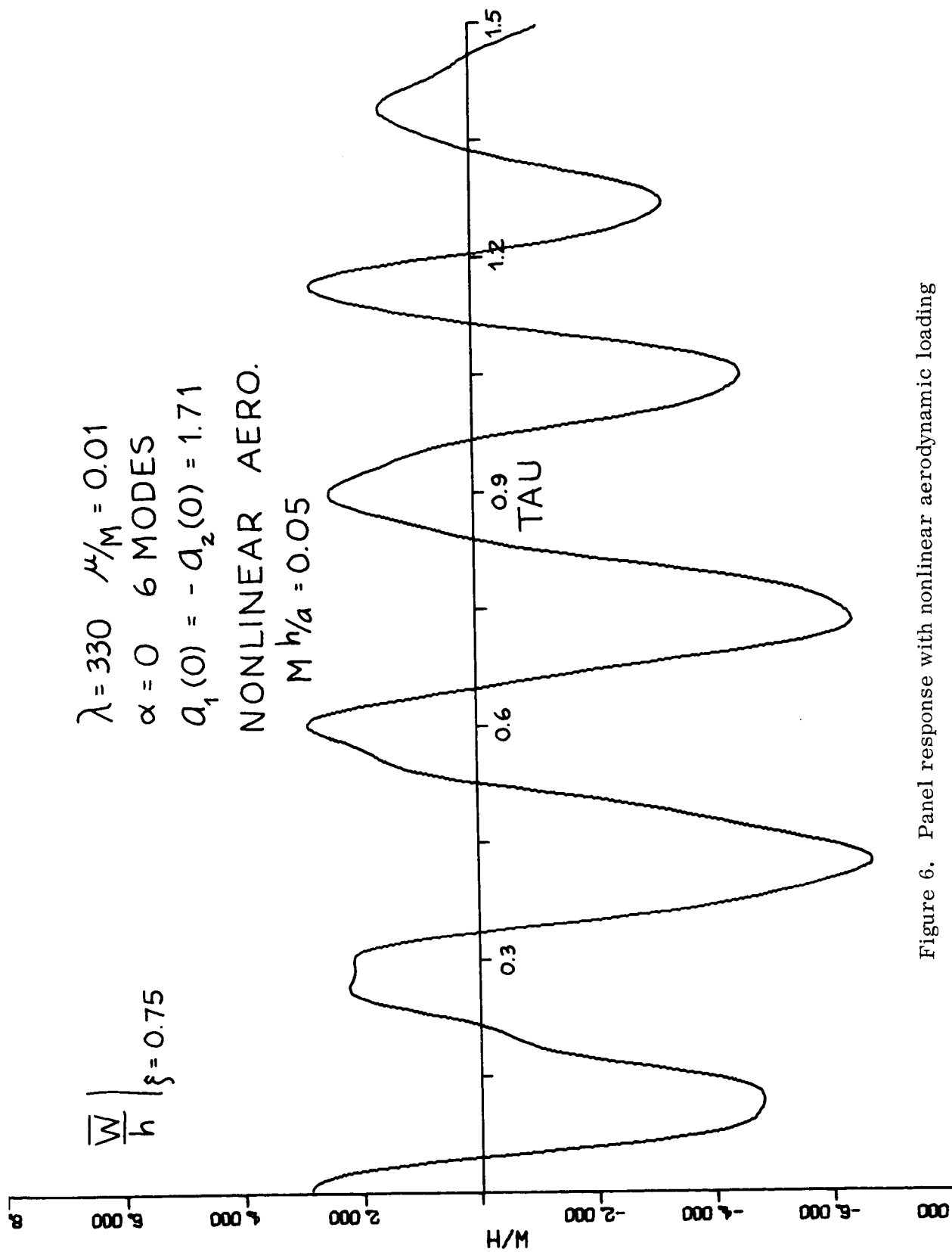


Figure 6. Panel response with nonlinear aerodynamic loading

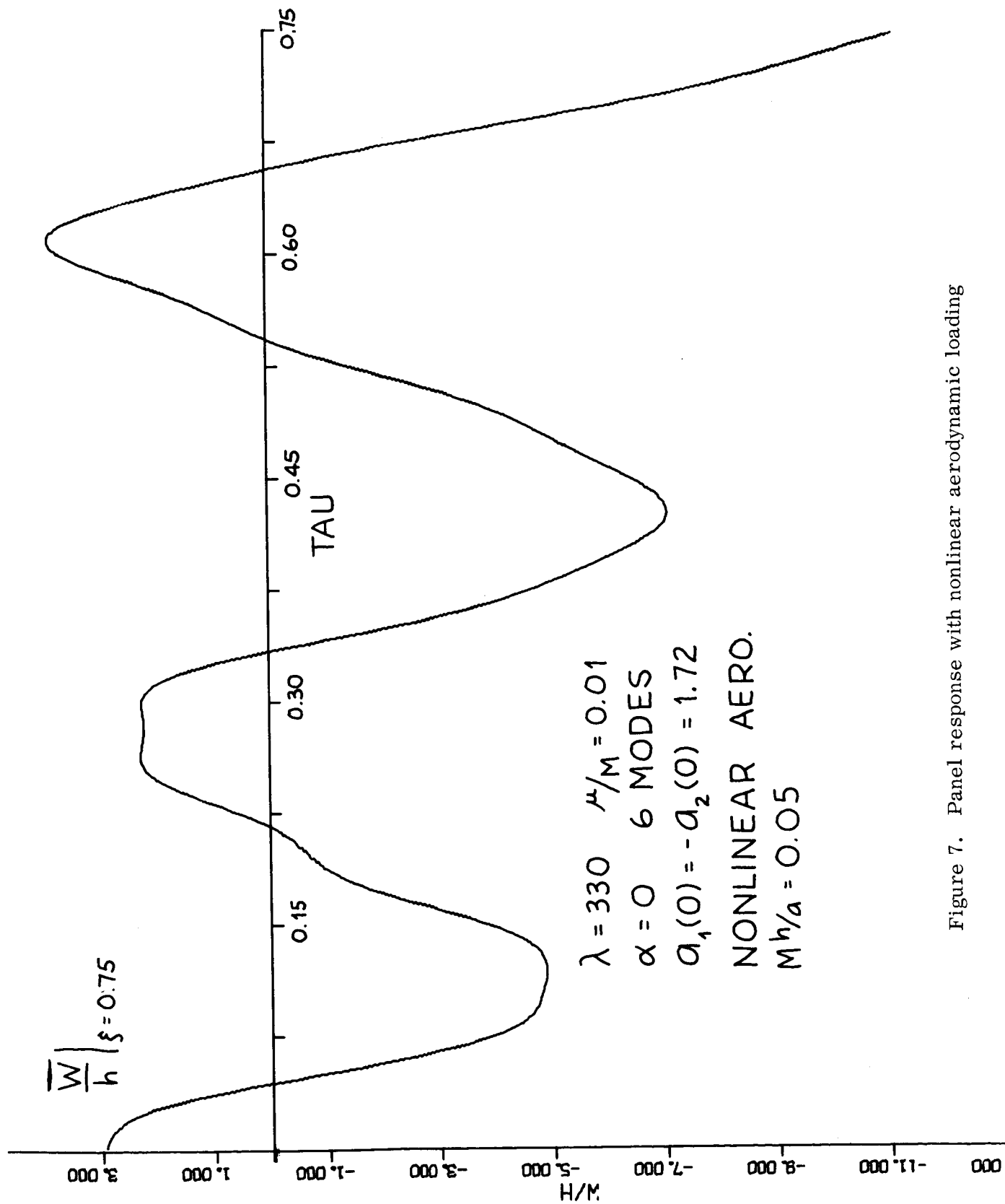


Figure 7. Panel response with nonlinear aerodynamic loading